ENERGY-SAVING TECHNOLOGIES AND EQUIPMENT

*For an electric power system (EPS) of the combined propulsion complex (CPC), working on a constant-power hyperbola (CPH), the strategy of managing power distribution between propulsion electric motors and own needs consumers has been improved. The study reported here aimed to reduce fluctuations in current consumption and load by optimizing voltage controllers and the rotation frequency of generator assemblies (GA). The system of EPS GA voltage and frequency stabilization was synthesized by determining, in the system of equations, the dynamics of the values of EPS links' time constants and the coefficients that correspond to control parameters. To define the characteristics of the control signals from the regulators of EPS GA rotation frequency and excitation voltage, the laws that control the speed and excitation current were calculated. After sampling the coefficients of the GA speed control regulator, the tasks for the excitation voltage controller were determined. The methodology of data acquisition was applied on the basis of a correlation between the EPS characteristics and the experimental characteristics of GA. The system of EPS dynamics equations was optimized in accordance with the structure and settings of the optimal controller and the probability of a situational error by using Spearman's rank correlation coefficient. The optimization has made it possible to reduce the likelihood of a situational error during the synchronization of GA and enable the stable operation of GA close to the mode of operation on CPH. The power controller was tested under the mode of changing the load of own needs with the power levels of EPS on CPH in the range of 50–100 % of the rated power. The range of deviations of the current consumed with an enabled GA rotation controller was 10 % of the average value. The range of EPS power deviations with the power controller turned on was 5 %*

*Keywords: electric power system, constant-power hyperbola, control system, optimization, correlation analysis*

# OPTIMIZATION OF THE CONTROL SYSTEM FOR AN ELECTRIC POWER SYSTEM OPERATING ON A CONSTANT-POWER HYPERBOLE

**Vitalii Budashko**
*Corresponding author*
Doctor of Technical Sciences, Professor
Educational and Scientific Institute of Automation
and Electromechanics*
E-mail: bvv@te.net.ua

**Albert Sandler**
Associate Professor
Department of Automatic Control Theory
and Computer Science*

**Valerii Shevchenko**
Doctor of Technical Sciences, Associate Professor
Department of Ships' Technical Operation*
*National University "Odessa Maritime Academy"
Didrikhsona str., 8, Odessa, Ukraine, 65029

## 1. Introduction

It is quite obvious that for the normal operation of an electric power system (EPS) of any complexity and structure, it is necessary to ensure the invariability of parameters of EPS operating generator assemblies (GAs), that is, the stability, first of all, of the voltage and frequency on the buses of the main switchboard (MSB). However, for a number of reasons, the voltage and frequency of generators tend to change [1]. A well-known fact is that, for example, short-circuit currents in the electric network are not precisely analyzed at an asymmetric voltage drop. The main difficulty is that the reaction and feedback of converters remain unclear at a partial drop in voltage [2]. It can be stated that scientific studies of voltage and frequency failures in short circuits are mainly associated with the distribution of the voltage of reverse sequence in windings and converter on the side of the excitation winding [3]. In this case, electromagnetic processes in the windings of generators and excitation control processes are simultaneously derived in a single coordinate space by constructing vector models of the direct and inverse sequence [4].

The main tools for studying the effects of voltage and frequency drop on load characteristics are Power Tools for Windows (PTW) software [5] and real-time digital simulator (RTDS) [6]. To perform the analysis of methodologies, Snapshot and Time-Domain software products, respectively [7]. Research can be carried out for differences regarding the parameters required for each methodology, with special applications for autonomous EPSs, which include synchronous generators (SGs) and powerful induction motors (IMs) [8].

However, in order to determine the operational properties, in particular, of autonomous EPSs, it is necessary to have tools for assessing and configuring additional parameters of voltage and frequency controllers equipped with electronic converters operating on a constant-power hyperbola (CPH) [9]. Improving voltage and frequency stability is based on the use of modeling in the PSCIM software. The proposed scenarios for modeling transients make it possible to achieve a reduction in voltage drop from 16 to 6 % and frequency surge – from 7 to 5 %.

On the other hand, all the latest approaches to managing voltage drop are based on the parameterization of controllers, which does not make it possible to separate the problem of

stability from the power balance [10]. The fact is that voltage drop regulation is usually used for a set limit and implies simple proportional control while the choice of frequency controller transfer coefficients is usually based only on power balance criteria. However, some values of the coefficients can cause poor damped response and even instability of EPS [11].

In [12], the authors note that in order to maintain the propulsion force, it is necessary to adjust the parameters of an autonomous EPS in parallel with maintaining the stability of the energy and motor system. In other words, that requires multi-level approaches to the management of electricity generation from researchers. To resolve the issue, it is necessary to first carry out mathematical modeling of each component in a power system, after which a common EPS is integrated into the format of the state space with the elements of model forecasting [13].

It can be summed up that studies related to ensuring the constant parameters of electric energy of EPS for various purposes are relevant. On the other hand, given the difficulties with structuring and settings of power distribution control systems, there is an issue related to assessing possible errors. This confirms the fact that the optimization of control systems is imperfect and, in some cases, can, in the long term, lead to an increase in inevitable losses.

## 2. Literature review and problem statement

Solutions to the task to stabilize electricity parameters of autonomous EPSs with the simultaneous preservation of the propulsion force range from improving the configuration and architecture to solutions for managing stabilization systems, in particular voltage and power frequency controllers. In the literature, several architectural solutions were proposed to improve the quality of electrical energy [14]. It was noted about the increase in the hardware complexity of power distribution systems with the dominance of converters due to the presence of a large number of renewable energy sources, energy storage systems, and energy-efficient loads leads to an improvement in the overall quality of electricity. However, as regards the structural energy efficiency index (coefficient) (SEEI) and a vessel's energy efficiency management plan (PVEEMP), there remain issues related to electricity quality indicators for EPS that require adjustments. This is especially important in terms of the causes and consequences of electricity quality problems in EPS, which must be taken into consideration at the design stage. In [15], the authors obtained the characteristics of power transfer processes in power supply systems and their control strategies in terms of improving efficiency with the addition of energy storage modules. As regards the methods of optimizing the parameters of EPS, the issues of their use as means of intelligent design to improve the performance of EPS remained unresolved. The issues of power supply systems management and load redistribution with centralized controllers and coordination at the system level through the use of distributed controls based on local information are discussed in [16]. However, the design of EPS with iterative adjustments to SEEI and VEEMP should take into consideration the energy from EES GA and the energy of load recovery, which is not possible without the appropriate optimization of control systems.

In [17], it was possible to take into consideration the impact of each component of EPS on its stability, using a multistage configuration, which includes the output cascade, the links of converters between the buses, and a general load cascade. However, it was stated that it is impossible to take into consideration the results of testing the proposed converter control systems at the EPS design stage since the controlled parameters change during the distribution of load capacity. The study of the strategy for mitigating voltage surges with the addition of resistive loads, filters, or energy storage devices directly connected to MSB, as well as methods for controlling these elements, is reported in [18]. It was noted that the advantages and disadvantages of those methods cannot be investigated without modeling and conducting appropriate hardware experiments. Impedance specifications and improved I/O impedance for converters and filters have been identified in [19] but only improving impedance at any link does not fully address the correlation between SEEI and the VEEMP of a particular vessel.

It can be concluded that the stages of correction of SEEI and VEEMP match certain studies with a certain degree of intercorrelation and the influence of some on others. In particular, stabilization of voltage and frequency on CPH Constant Power Loads (CPL) has been studied in many research papers. For example, paper [20] investigated the stability of autonomous EESs operated on CPH under the influence of a non-deterministic perturbation, where it is assumed that the power supply of EPS varies. The reported results clearly indicate that additional adjustment flexibility is needed to enable the stable operation of EPS in the case of critical situational errors. The study is presented as a stage of correction of PVEEMP in terms of overcoming the new safety problem of an autonomous EPS, which does not contain only technical solutions, that is, at the stage of correction of SEEI. As regards PUEES, work [21] analyzes the stability of EPS with converters on the DC-Link line, and then two linear control approaches are proposed to stabilize the power voltage as part of SEEI improvement. In [22], the ambiguous nature of programming approaches, as an element of design solutions used to analyze the stability and control of EPS, is indicated as a self-sufficient problem. This, in turn, accumulates [23] existing methods of compensating for voltage drop on the methods of using cascading power converters with a warning perturbation controller.

As regards the analysis of circuitry as a component of the improvement of SEEI, most EPSs consist of several GAs, energy storage systems (ESSs), and fuel cells that are connected in a network through power converters. The various perturbing forces acting on GA turn EPS into a time-distributed system, so taking this factor into consideration from the point of view of VEEMP is very problematic. Dynamic modeling of such EPSs is investigated in [24] but the accuracy of parameterization of models primarily affects SEEI and not VEEMP. On the other hand, resistance to frequency failure [25] is achieved through the use of real-time load management techniques, which is the stage of correction of VEEMP, due to which the probability of erroneous diagnosis and erroneous calculation decreases. To stabilize the EPS parameters, decentralized, distributed, and hierarchical control approaches are used. In [26], to achieve voltage stability, a distributed control approach is proposed by monitoring the state of the ESS charge. At this stage, the functional description of the EPS elements remains limited, which creates difficulties in building hierarchical management structures. And although in [27] a dc-link voltage is controlled using a hierarchical control scheme in the presence of energy storage modules and renewable energy sources, the goal of adjusting VEEMP is not fulfilled. To ensure the stability of EPS by controlling the generated direct current of power sources,

paper [28] proposes a decentralized control approach that is effective only at the stage of structural adjustments. Therefore, work [29] analyzes and compares the configuration and characteristics of multilevel control systems for sequential, parallel, and sequentially parallel hybrid power systems. As a result, the recommendations were proposed only to improve reliability, control, and efficiency in the process of building multi-level energy systems for large-tonnage vessels.

Over the past few years, improved and new management strategies have been adopted for autonomous EPSs by designers and researchers, which, to some extent, have made it possible to improve SEEI and more accurately build VEEMP. For example, paper [30] uses a distributed adaptive control approach to EPS and then investigates and studies the interaction between embedded AC and DC networks. However, the main key technology, which has not yet been fully considered, is the dynamic and distributed VEEMP, monitoring and management of disparate and interacting elements of ESS. The decision support and management systems for multilevel autonomous electricity converters discussed in [31] contribute to solving these problems but do not completely eliminate them. Local problems, such as the adjustment of voltage and rotation frequency of diesel generators [32], are solved by linearized control methods with integrated feedback and control of CPH charge without taking into consideration VEEMP. Methods of predictive management of automatic voltage controllers of EPS, which feed, in particular, energy-saving powerful electric drives, are used [33] but, to date, are not unified, and cannot be considered as universal in terms of improving the SEEI.

In all the reviewed body of research, the circuitry-based correction of VEEMP is carried out locally, at the level of active correction of the managed signal error. That is, in the energy conversion chain, there is a controller that divides the stage of regulation of the controlled parameter into, in fact, the regulatory process itself and the process of error prevention. However, compared to passive uncontrolled converters, active ones are more expensive, require more maintenance, and have greater design characteristics. In addition, in the scientific literature, studies into the stability of EPS as a component of VEEMP are limited compared to the control over energy consumption, which is laid down by SEEI [34, 35]. There are no agreements on the mandatory application or establishment of the necessary objectives and performance studies. Today, there are no detailed specific measures to be implemented while the costs associated with the new requirements for SEEI and VEEMP can be justified on one basis or another. Note that one of the main disadvantages of EPS for hybrid (combined) propulsion complexes is, to date, the lack of appropriate universal control methods. For EPSs working on CPH, firstly, it is possible to unify control methods, and, secondly, to reduce the number of design iterative procedures. Such control methods are based on controllers of different levels, that is, the "sets" of coordinated signals directly depend on the structure of EPS, the development of functional relationships between elements [36], which, in turn, gives rise to situational errors.

In general, the procedure for compiling a list of situational errors is based on an analysis of the functioning of the involved information devices and EPS control signals. It is to be determined whether a given control signal can be used in solving a specific problem. Once it can, then the assessment of this situation is carried out in the list of inspections. In the case it cannot, then it is checked whether a situational error is missed in this case and which signal is used as an intermediate.

Summing up, it can be concluded that the structural energy efficiency index (SEEI) and a vessel's energy efficiency management plan (VEEMP) directly depend on the structural and characteristic parameters of EPS control systems, in particular, those operating on CPH. There are mechanisms that have been implemented over the past few years. There are many ways to optimize energy transfer control systems on-board a ship; they can be divided into technical and structural aspects based on the operational and maintenance factors. Therefore, measures to optimize the control systems of EPS operating on CPH represent a relevant issue that requires general and partial solutions in the design of environmentally friendly, energy-efficient, and inexpensive options.

## 3. The aim and objectives of the study

The purpose of this study is to synthesize a system for stabilizing the voltage and frequency of EPS generator assemblies with optimal control over combined propulsion complexes (CPC) that operate on constant-power hyperbola. This will make it possible to minimize the deviation of the parameters of the electric power system and control signals if a situational error appears.

To accomplish the aim, the following tasks have been set:
– to optimize the systems of EPS dynamics equations in accordance with the structure and settings of the optimal controller and the likelihood of a situational error;
– to estimate the variances of deviations of the parameters of the electric power system and control signals if a situational error appears.

## 4. The study materials and methods

It is known from [37] that the optimal load of the EPS operator is in the region $H = 0,53$. If one determines, for this region, the probability of a situational error, then to assess the logical complexity and stereotyping of control algorithms, it is necessary to normalize the corresponding coefficients $L_H$ i $Z_H$ by calculating them as follows:

$$m_0 = m_C + m_M; \quad n_0 = n_C + n_M,$$

$$S_k = \frac{m_L}{m} \sum_{k=1}^{g_L} \frac{n_L^2(k)}{n(k)}; \quad P_k = \frac{m_0}{m} \sum_{k=1}^{g_0} \frac{n_0^2(k)}{n(k)}, \qquad (1)$$

where $m_L$, $m_C$, $m_M$ is the number of logical, sensory, and motor action operators in the control algorithm; $m$ is the total number of operators; $n_L$, $n_C$, $n_M$ is the number of logical, sensory, motor action operators in the $k$-th group of the algorithm, depending on the structure of EPS; $n$ is the total number of operators in the $k$-th group; $g_L$, $g_0$ is the number of groups in the control algorithm.

The accuracy of adjusting the voltage and frequency of GA on CPH in the presence of optimal regulators is determined by variance in the adjusted value. The GA voltage variance when adjusting the excitation current in the load current function for th predefined full power $S$ is written as [38]:

$$D_u = \int_0^\infty \left| \frac{c + j\omega_{dg} d}{Y(j\omega_{dg})} \right|^2 S_\mu(\omega_{dg}) d\omega, \qquad (2)$$

where the output vector $Y$ of the model of CCP EPS is constructed in the form of a regression equation in the presence of a matrix of observations $X$; $\omega_{dg}$ is the GA shaft rotation frequency;

$$X = \begin{bmatrix} x_{11} & x_{12} & ... & x_{1n} \\ x_{21} & x_{22} & ... & x_{2n} \\ .. & .. & .. & .. \\ x_{N1} & x_{N2} & ... & x_{Nn} \end{bmatrix}; \quad Y = \begin{bmatrix} y_1 \\ y_2 \\ . \\ . \\ . \\ y_N \end{bmatrix}. \quad (3)$$

Moreover, the studied EPS control system is a system with two inputs and two outputs. In this case, it is advisable to use strategies known as I/O, in which I/O responses are also split. The system must be linearized if the vector of relative degrees of linearization $\{r1, r2\}$ exists under the following conditions:

$$X_i Y_f^k y_i(x) = 0$$

for all $1 \le i, j \le 2$ and $k \le r_i - 1$, where $X_s R(x) = \dfrac{d}{dx} R(x) \times Y$, which is derivative $R$ in the direction of $S$.

The stable subfamily of solutions to equation (2) for task $\mu(t)$ satisfies the equation with respect to the outputs of the model:

$$Y(p)i = \frac{X(-p)F(p)}{Y(-p)}\mu, \quad (4)$$

taking into consideration the properties of the function, the task $\mu(t)$ is written as:

$$Y'(p)i = \frac{X(-p)F(p)}{Y(-p)}\mu = (K_1 + jK_2)\mu = (c + dp)\mu, \quad (5)$$

where, taking into consideration (2):

$$c = k_1 + \delta_{dg}k_2 / \omega_{dg}, \, d = k_2 / \omega_{dg};$$

$\delta_{dg}$ is the GA load angle.

Taking into consideration the stochastic nature of the disturbances that act on the CPC EPS, it is necessary to limit the task relative to the established point, that is: the decoupling matrix $\Delta(x)$ must be undegenerated around the established point of the system $x_0$:

$$det(\Delta(x)) \ne 0$$

where

$$|x - x_0| \le 0,$$

where

$$\Delta(x) = \begin{bmatrix} X_{g1}Y_f^{r_1-1}y_1(x) & X_{g2}Y_f^{r_1-1}y_1(x) \\ X_{g1}Y_f^{r_2-1}y_2(x) & X_{g2}Y_f^{r_2-1}y_2(x) \end{bmatrix}. \quad (6)$$

By sequentially applying a derivative output system considering $(x)$, a vector of relative degrees equal to $\{2, 2\}$ is calculated. As a result, taking into consideration the above conditions, a decoupling matrix $A(x)$ is built:

$$\Delta(x) = \begin{bmatrix} \dfrac{1}{H}S_R^{r_i}X_R^{r_i}Y_1X_R^{-1}\text{ш}_{dg} & \dfrac{k_{ij}}{2H} \\ \dfrac{S_R^{r_i}Y_2X_R^{-1}\text{ш}_{dg}}{c\sqrt{S_R^{r_i}Y_2S_R}} & 0 \end{bmatrix}, \quad (7)$$

where $H$ is the constant of GA inertia.

The decoupling matrix is not special next to the established point (points) of the set of control tasks. It should be emphasized that $\|x_0\| \ne 0$.

If we set the value $S_\mu$ (2) and exclude the function $\mu(t)$ from equations (4), (5), we obtain:

$$[X(p)(c + dp) - F(p)Y(p)]i = -B(p)(c + dp)u_i, \quad (8)$$

hence, the equation of a stable optimal excitation current controller of EPS GA takes the form:

$$u_i = \left[ \frac{Y(p)f(p)}{B(p)(c + dp)} - \frac{X(p)}{B(p)} \right], \quad (9)$$

and the equation of the optimal power controller, derived similarly, is written as:

$$U(p) = \left[ \frac{G(p)}{N(p)} - \frac{Z(p)R(p)}{N(p)(U + \omega p)} \right] S_R. \quad (10)$$

The equations of optimal controllers of excitation currents depending on the scheme of the main GA circuit are identical, due to the identity of the GA dynamics equation system. The equations of the optimal controller of EPS unchanging power, which affects, for example, the controlled rectifier of the main circuit (subject to its presence in the main current circuit), are derived similarly to (9) and (10). Such transformations are possible because the time constant of any electrical converter is less than the total $H$.

## 5. Results of studying the optimization of the control system in an electric power system operating on a constant-power hyperbola

### 5. 1. Dynamic structuring of the equation system and setting up the optimal controller for an electric power system

The states of energy conversion systems with two inputs $(u, f)$ and two outputs $(\omega_{dg}, \delta_{dg})$ in the chain "GA – load" are calculated from equations (5) to (7):

$$\zeta_1^1 = y_1 = h_1(x);$$

$$\zeta_2^1 = \dot{y}_1 = X_{(f+g_1u_1+g_2u_2)}h_1(x);$$

$$\zeta_3^1 = \dot{\upsilon}_1 = X_{(f+g_1u_1+g_2u_2)}^2 h_1(x);$$

$$\zeta_1^2 = y_2 = h_2(x);$$

$$\zeta_2^2 = \dot{y}_2 = X_{(f+g_1u_1+g_2u_2)}h_2(x);$$

$$\zeta_3^2 = \dot{\upsilon}_2 = X_{(f+g_1u_1+g_2u_2)}^2 h_2(x);$$

where $\upsilon_1$ and $\upsilon_2$ are the system inputs for EPS energy conversion (Fig. 1).

In Fig. 1, the reference value of the torque on the shaft of the propulsion electric motors $M_d$ is calculated on the basis of the dynamic parameters of a vessel and the structural characteristics of propellers [39]:

$$T_d = h_T(n,x,\theta)(1-t)T_p =$$
$$= f_T(n,x,\theta),$$

$$M_d = h_F(n,x,\theta)F_p =$$
$$= f_F(n,x,\theta),$$

where $x$ is the dynamic parameters of the vessel; $\theta$ is the dependent parameters of propellers.

A relationship between the inputs of the control system of optimal controllers $u_1$ and $u_2$ and the inputs of energy conversion of EPS running on CPH can be written as:

$$\begin{bmatrix} u_1 \\ u_2 \end{bmatrix} = -\Delta^{-1}(x)\begin{bmatrix} X_f^2 y_1 \\ X_f^2 y_2 \end{bmatrix} + \Delta^{-1}(x)\begin{bmatrix} \upsilon_1 \\ \upsilon_1 \end{bmatrix}. \tag{11}$$

Thus, the separated control systems for optimal controllers take the following form:

$$\begin{bmatrix} \dot{\zeta}_1^1 \\ \dot{\zeta}_2^1 \end{bmatrix} = \begin{bmatrix} 0 & 1 \\ 0 & 0 \end{bmatrix}\begin{bmatrix} \dot{\zeta}_1^1 \\ \dot{\zeta}_2^1 \end{bmatrix} + \begin{bmatrix} 0 \\ 1 \end{bmatrix}\upsilon_1;$$

$$\begin{bmatrix} \dot{\zeta}_1^2 \\ \dot{\zeta}_2^2 \end{bmatrix} = \begin{bmatrix} 0 & 1 \\ 0 & 0 \end{bmatrix}\begin{bmatrix} \dot{\zeta}_1^2 \\ \dot{\zeta}_2^2 \end{bmatrix} + \begin{bmatrix} 0 \\ 1 \end{bmatrix}\upsilon_2.$$

In order to stabilize the EPS operating on CPH under a certain operational mode, feedback is established to stabilize the state, which takes the following form:

$$\upsilon_1 = -k_{11}(\zeta_1^1 - \omega_{ref}) - k_{12}\zeta_2^1;$$
$$\upsilon_2 = -k_{21}(\zeta_1^2 - u_{ref}) - k_{22}\zeta_2^2, \tag{12}$$

where $\omega_{ref}$ and $u_{ref}$ are the GA shaft rotation frequency and the excitation voltage, respectively. The coefficients $k_{11}$, $k_{12}$, $k_{21}$, and $k_{22}$ correspond to the feedback control parameters.

For example, for GA with an independent excitation winding, parameters for control tasks $\mu(t)$ (4) in accordance with the transfer coefficients $k_{11}$, $k_{12}$, $k_{21}$, and $k_{22}$ (Fig. 1) are found as follows:

$$\alpha(\delta_{dg}, \omega_{dg}, U_{dg}, I_{dg}) =$$
$$= \mu_0 + \mu_1\delta_{dg} + \mu_2\delta_{dg}^2 + \mu_3\delta_{dg}^3, \tag{13}$$

$$\beta_f\begin{pmatrix} \delta_{dg(f)}, \omega_{dg(f)}, \\ U_{dg(f)}, I_{dg(f)} \end{pmatrix} =$$
$$= \mu_0^* + \mu_1^*\delta_{dg} +$$
$$+ \mu_2^*\delta_{dg}^2 + \mu_3^*\delta_{dg}^3. \tag{14}$$

Then, for the transfer coefficients $k_{11}$, $k_{12}$, $k_{21}$, and $k_{22}$, we determine the power value on CPH as follows:

$$S_f(z_2^1(N)) \leq (\dot{\zeta}_1^1(N) - \omega_{ref}^j(N))^2. \tag{15}$$

After the transformations, taking into consideration (12), we obtain an expression for iterative procedures for determining the power:

$$S(\zeta_1^j(k_i), \omega_{ref}^j(k_i), \upsilon_1^j(k_i)) =$$
$$= \alpha(\zeta_1^j(k_i) - \omega_{ref}^j(k_i))^2 - \beta(\upsilon_1^j(k_i))^2, \tag{16}$$

where the non-negative parameters $\alpha$ and $\beta$ are the weights characterizing certain operational factors for the power values on CPH.

In the cases of inaccessibility of model parameters or the impossibility to identify and measure them, the data must be filtered by the criterion of significance to a certain operational situation in terms of avoiding situational errors. Then, in accordance with (12), significance coefficients will be calculated taking into consideration the integral condition for controlling the voltage and rotation frequency. For such cases, the integral component must be taken into consideration in the control system:

$$\upsilon_1 = -k_{11}(\zeta_1^1 - \omega_{ref}) -$$
$$- k_{11}^*\int_0^t(\zeta_1^1 - \omega_{ref})dt - k_{12}\zeta_2^1;$$

$$\upsilon_2 = -k_{21}(\zeta_1^2 - u_{ref}) -$$
$$- k_{21}^*\int_0^t(\zeta_1^1 - \omega_{ref})dt - k_{22}\zeta_2^2, \tag{17}$$

where $k_{11}^*$ and $k_{21}^*$ are the control system configuration constants associated with the cumulative error period.
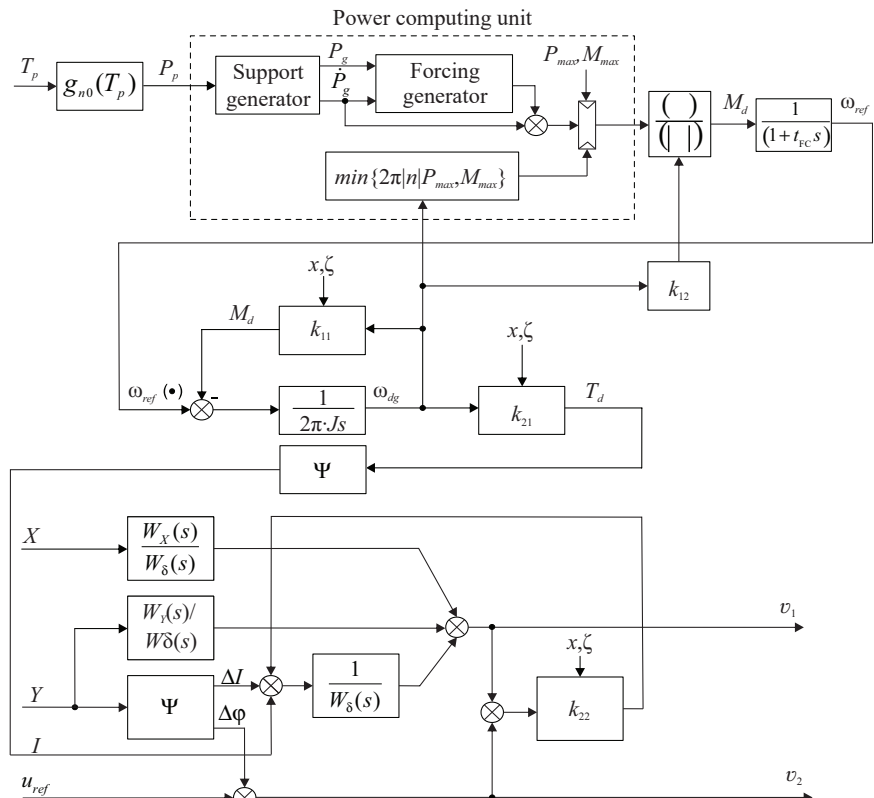


Fig. 1. Flowchart of the control strategy for an electric power system operating on a constant-power hyperbola

Studies in this area have proven that the specified parameters are the functions of the GA load angle $\delta_{dg}$, the rotation frequency of the GA shaft $\omega_{dg}$, the GA voltage $U_{dg}$, and the GA active current $I_{dg}$, respectively, on the circuits of the stator and excitation:

$$\alpha = \alpha\left(\delta_{dg}, \omega_{dg}, U_{dg}, I_{dg}\right),$$

$$\beta = \beta_f\left(\delta_{dg(f)}, \omega_{dg(f)}, U_{dg(f)}, I_{dg(f)}\right).$$

Usually, such functions are approximated by approximate polynomials. Taking into consideration (16), we obtain:

$$\alpha\left(\delta_{dg}, \omega_{dg}, U_{dg}, I_{dg}\right) =$$
$$= \sum_{i=k}^{k+N-1} S_k\left(\dot{\zeta}_1^{\lambda_k}(i), \omega_{ref}^{\lambda_k}(i), \upsilon_1^{\lambda_k}(i)\right) + S_f\left(\dot{\zeta}_1^{\varphi_k}(k+N)\right), \quad (18)$$

$$\beta_f\left(\delta_{dg(f)}, \omega_{dg(f)}, U_{dg(f)}, I_{dg(f)}\right) =$$
$$= \sum_{i=k}^{k+N^*-1} P_k\left(\dot{\zeta}_1^{\lambda_k}(i), \omega_{ref}^{\lambda_k}(i), \upsilon_1^{\lambda_k}(i)\right) + P_f\left(\dot{\zeta}_1^{\varphi_k}(k+N^*)\right), \quad (19)$$

where the number of terms $N$, $N^*$ and the indicators of powers $\lambda_k$, $l_k$, $\sigma_k$, $\varphi_k$, and the values of $S_k$, $P_k$ in (18), (19) depend on the structural characteristics of GA and are determined by the correlation method based on the results of the processing of experimental data.

Within a certain operating mode for power on CPH that does not exceed the rated values, we obtain a ratio for control tasks $\mu(t)$

$$\mu_0 = S_1 + S_2 U_{dg} + S_4 U_{dg}^2 + S_6 \omega_{dg} U_{dg}^2 + S_8 I_{dg} +$$
$$+ S_9 U_{dg} I_{dg} + S_{11} \omega_{dg} I_{dg} + S_{12} U_{dg}^3 + S_{14} U_{dg}^6 + S_{16} \omega_{dg}^2 +$$
$$+ S_{20} U_{dg}^3 I_{dg} + S_{24} \omega_{dg} U_{dg}^3 I_{dg} + S_{27} \omega_{dg}^2 U_{dg}^3 I_{dg} +$$
$$+ S_{29} I_{dg}^2 + S_{34} \omega_{dg} I_{dg}^2 + S_{36} \omega_{dg} U_{dg}^3 I_{dg}^2 + S_{40} \omega_{dg}^2 U_{dg}^3 I_{dg}^2;$$

$$\mu_1 = S_5 \omega_{dg} U_{dg} + S_{15} U_{dg} I_{dg} + S_{18} \omega_{dg} I_{dg} +$$
$$+ S_{22} \omega_{dg}^2 U_{dg}^3 + S_{26} U_{dg}^3 I_{dg} + S_{28} \omega_{dg}^2 I_{dg} +$$
$$+ S_{31} I_{dg}^2 + S_{33} U_{dg}^3 I_{dg}^2 + S_{37} U_{dg}^6 I_{dg}^2 + S_{39} \omega_{dg} U_{dg}^6 I_{dg}^2;$$

$$\mu_2 = S_3 I_{dg} + S_{10} U_{dg}^6 + S_{17} \omega_{dg}^2 +$$
$$+ S_{21} \omega_{dg}^2 U_{dg}^6 + S_{32} I_{dg}^2 + S_{35} U_{dg}^6 I_{dg}^2;$$

$$\mu_3 = S_{13} \omega_{dg} + S_{19} \omega_{dg}^2 + S_{23} U_{dg}^6 I_{dg} +$$
$$+ S_{25} I_{dg}^2 + S_{30} U_{dg}^3 I_{dg}^2 + S_{38} \omega_{dg} U_{dg}^6 I_{dg}^2;$$

$$\mu_0^* = P_0 + P_3 U_{dg}^2 + P_6 \omega_{dg} U_{dg} + P_9 \omega_{dg} U_{dg}^2 +$$
$$+ P_{11} U_{dg} I_{dg} + P_{14} \omega_{dg} U_{dg}^2 I_{dg} + P_{18} \omega_{dg} U_{dg}^3 +$$
$$+ P_{20} \omega_{dg}^2 + P_{23} \omega_{dg}^2 U_{dg} + P_{26} \omega_{dg}^2 U_{dg}^3 + P_{29} \omega_{dg}^2 U_{dg}^6 +$$
$$+ P_{32} U_{dg}^6 I_{dg} + P_{34} \omega_{dg} U_{dg}^6 I_{dg} + P_{36} \omega_{dg}^2 U_{dg}^2 I_{dg} +$$
$$+ P_{38} \omega_{dg}^2 U_{dg}^6 I_{dg} + P_{40} \omega_{dg} U_{dg}^3 I_{dg}^2 + P_{43} \omega_{dg} U_{dg}^6 I_{dg}^2 +$$
$$+ P_{45} \omega_{dg}^2 I_{dg}^2 + P_{47} \omega_{dg}^2 U_{dg}^3 I_{dg}^2 + P_{49} \omega_{dg}^2 U_{dg}^6 I_{dg}^2;$$

$$\mu_1^* = P_2 U_{dg} + P_5 \omega_{dg} U_{dg} + P_{10} I_{dg} + P_{12} U_{dg} I_{dg} +$$
$$+ P_{15} \omega_{dg} U_{dg} I_{dg} + P_{19} \omega_{dg} U_{dg}^3 + P_{21} \omega_{dg}^2 + P_{27} \omega_{dg}^2 I_{dg} +$$
$$+ P_{31} U_{dg} I_{dg}^2 + P_{37} \omega_{dg} I_{dg}^2 + P_{44} \omega_{dg}^2 U_{dg}^6 I_{dg}^2;$$

$$\mu_2^* = P_1 + P_4 \omega_{dg} U_{dg} + P_{13} U_{dg} I_{dg} + P_{16} \omega_{dg} I_{dg} +$$
$$+ P_{25} \omega_{dg}^2 U_{dg}^2 + P_{33} \omega_{dg}^2 U_{dg}^6 +$$
$$+ P_{39} \omega_{dg}^2 U_{dg}^3 + P_{41} \omega_{dg}^2 U_{dg}^3 I_{dg}^2 + P_{42} \omega_{dg}^2 U_{dg}^3 I_{dg};$$

$$\mu_3^* = P_7 \omega_{dg} + P_8 \omega_{dg}^2 + P_{17} \omega_{dg} U_{dg}^2 + P_{22} I_{dg} +$$
$$+ P_{24} U_{dg}^6 I_{dg} + P_{28} \omega_{dg} I_{dg} + P_{48} \omega_{dg}^2 U_{dg}^3 I_{dg}^2;$$

$S_k$ and $P_k$ (1) values are determined by data sets based on the results of iterative calculations of the transfer coefficients $k_{11}$, $k_{12}$, $k_{21}$, and $k_{22}$, which enable the steady state of the control system of EPS GA on CPH:

$$\{S_k\}_{\overline{k=0;40}} =$$
$$= \left\{ \begin{array}{l} 0.2164825; -0.219488; 0.276264; \\ 0.268113; -0.137651; -0.552797; \\ 0.19116428; 0.0143051; -0.1921055; \\ 0.1132481; 0.1413526; -0.0126594; \\ 0.1109689; -0.148498; 0.02725307; \\ -0.01148727; 0.278496, -0.1307277; \\ 0.0863669; -0.1919475; 0.01345252; \\ -0.00842128; 0.0165324; \\ -0.1981791; 0.018619; -0.19110598; \\ -0.001325238; -0.00595519; \\ -0.0019896; -0.0024982; -0.001361325; \\ -0.001626652; -0.001988757; \\ 0.000114648; 0.001390941; 0.01921849; \\ 0.0001366481; -0.00136523 \end{array} \right\};$$

$$\{P_k\}_{\overline{k=0;49}} =$$
$$= \left\{ \begin{array}{l} 0.0279255; -0.0876648; -0.198231; \\ 0.0243765; -0.4108511; -0.108009; \\ -0.0586281; 0.278661; -0.0270871; \\ 0.0412595; 0.0209459; 0.0323219; \\ -0.0748408; 0.0328258; -0.0269402; \\ 0.1368052; 0.0161886; 0.0216285; \\ 0.027894; 0.1972729; 0.0196282; \\ -0.1302782; -0.020136; 0.4121148; \\ -0.0295748; -0.0260024; -0 / 0105823; \\ -0.0110902; -0.0212912; \\ 0.0025986; -0.0142121; -0.0252627; \\ 0.0126802; -0.0218258; 0.0224268; \\ -0.0152391; 0.0000122461; -0.0000297488; \\ 0.00259561; 0.000084866; \\ 0.0166485; 0.00202552; \\ -0.00001356; -0.0000325299; \\ 8.49242 \times 10^{-6}; -3.669 \times 10^{-4}; 6.33193 \times 10^{-6} \end{array} \right\}.$$

The basic technical and dynamic parameters of some types of GAs necessary for the construction of elemental mathematical models, taking into consideration the values of the coefficients in (18), (19), are given in Table 1.

In Table 1 (in accordance with (18) and (19):

– $\lambda = M_{\max}/M_N$ – overload capacity;

– $\sigma$ – the air gap between the stator and the rotor;

– $l$ – estimated length of the stator core;

– $\varphi$ – coefficient characterizing the inductive resistance of the winding scattering;

– $\sin\delta_{nom}$ and $\sin2\delta$ – parameters characterizing magnetic saturation under a rated mode and a mode with forcing excitation, respectively;

– $\gamma$ – the coefficient of mutual induction, which characterizes the overlapping of the stator windings.

Table 1

### GA technical and dynamical parameters

| GA | DG with AVC | TG with AVC | BL DG | BL TG | SG with AVC | BL SG |
|---|---|---|---|---|---|---|
| No. of entry | 1 | 2 | 2 | 5 | 4 | 6 |
| $U$ | LV | LV | HV | HV | LV | HV |
| $P$, W | $0\div1\times10^3$ | $1\div2\times10^3$ | $2\div5\times10^3$ | $2\div5\times10^3$ | $1\div2\times10^3$ | $2\div5\times10^3$ |
| $\varphi$ | 0.0421 | 0.0451 | 0.08089 | 0.0531 | 0.082 | 0.07441 |
| $\sigma$ | 1.718 | 1.8 | 1.55 | 1.6 | 1.2 | 1.9 |
| $l$ | 2.36 | 2.86 | 3.48 | 3.36 | 3.47 | 3.45 |
| $\omega_{dg}$ | 330 | 570 | 500 | 750 | 300 | 300 |
| $\delta_{dg(\max)}$ | 53 | 45 | 58 | 43 | 52 | 55 |
| $\sin\delta_{nom}$ | 0.934 | 0.812 | 0.821 | 0.916 | 0.913 | 0.8829 |
| $\sin2\delta$ | 0.946 | 0.832 | 0.849 | 0.973 | 0.982 | 0.9129 |
| $\gamma$ | 0.9812 | 0.9323 | 0.9609 | 0.974 | 0.988 | 0.9796 |
| $\mu_0$ | 0.3666 | 0.4559 | 0.2948 | 0.219 | 0.3514 | 0.3357 |
| $\mu_1$ | −0.2665 | −0.2632 | −0.2182 | −0.2613 | −0.1862 | −0.2475 |
| $\mu_2$ | −0.2423 | −0.266 | −0.2183 | −0.2612 | −0.4817 | −0.4885 |
| $\mu_3$ | 0.0839 | 0.08465 | 0.133 | 0.0747 | 0.132 | 0.0823 |
| $\mu_0^*$ | 0.051 | 0.13341 | 0.0276 | 0.0208 | 0.0269 | 0.0246 |
| $\mu_1^*$ | −0.0269 | −0.4171 | −0.1984 | −0.0282 | −0.0234 | −0.0287 |
| $\mu_2^*$ | −0.4130 | −0.427 | −0.0085 | −0.0219 | −0.0098 | −0.0241 |
| $\mu_3^*$ | −0.1979 | −0.05624 | −0.4107 | −0.1984 | −0.1313 | −0.025 |

For our experiment, we chose the EPS equipped with diesel generators (DG) and automatic voltage controllers (AVC). A short period of time was considered when a vessel moved at different speeds, which predetermined the necessary power to enable its movement and appropriate power adjustment on CPH. The reference voltage on the DC link was 560 V. In addition, the reference speed selected for EPS GA was $\omega_{ref}=30$ rev/s at the EPS frequency of 60 Hz. In this experiment, it is assumed that a load of own needs accounts for 20 % of the generated power. It is assumed that the time constants of the controllers are 10 ms (to power the propulsion electric motors and the GA excitation system). The results of the modeling are shown in Fig. 2.

To assess the logical complexity and stereotyping of control algorithms, it is necessary to normalize the corresponding coefficients $L_H$ and $Z_H$ (1). Another way is research based on the analysis of the correlation between two data streams: the characteristics of EPS and the moment of error. The data of the study are synchronized by time. To identify the significance of the correlation, it is necessary to calculate the values of the paired coefficients of Spearman [40], Pearson, or Kendall, as well as the levels of significance for them. Correlations measure the relationship between the variable characteristics of EPS and the ranks of the onset of the error. Before calculating the corresponding correlation coefficients, it is necessary to check

the data for situational errors (which can lead to misleading results) and signs of a linear relationship. Pearson's correlation coefficient is a measure of the linear relationship. Two variables can be 100 % related, but if this relationship is nonlinear, Pearson's correlation coefficient is not a suitable statistic for measuring it. Kendall's rank correlation coefficient is an alternative to Spearman's correlation method but it is designed to determine the relationship between two rank variables. That is, in the case under consideration, the rank correlation is more suitable for assessing the occurrence of two situational errors. Interpretation of the results of the calculation – Kendall's rank correlation coefficient is defined as the difference in the probabilities of coincidence and inversion in the ranks of situational errors. For example, estimates of the "drop" of EPS GA from synchronism and errors in measuring the rotation frequency of the propulsion electric motor or sudden loading. For the same values of variable characteristics of EPS, the value of the Spearman correlation coefficient will be slightly greater than the value of the Kendall rank correlation coefficient while the level of significance will be almost the same.

Based on this, the assessment of the relationship between the change of two values and the occurrence of a GA synchronization error is carried out using Spearman correlation coefficients. This is possible in cases where the measurement of the parameters of the studied EPS will be subject to the order in the appropriate scale, or the form of interrelation will differ from the linear one (Fig. 2). According to its calculation, it is necessary to arrange the sample options or, in other words, to group the experimental data in a certain order, either ascending or descending.

The homoscedasticity of the data was assessed as the absence of heteroscedasticity based on the analysis of the dependent characteristics of EPS (Fig. 2) and independent variables (the power of own needs). The data for dependent characteristics were arranged from smaller to larger with the rejection of values that were contained inside the ordered series. After calculating the residues and their squares of residual variances by distributions (20) and (21), their ratio was found. Comparing the found criteria with the critical value of the Fisher's $F$-criterion at the selected degrees of freedom and confidence level has proven that the output data did not demonstrate heteroscedasticity.

The load current manifests itself as a disturbance that occurs during the calculation of the transformed states of the system, that is, the states of linearly converted systems depend on the load current. The load current was measured not only by current sensors but was also assessed using the efficiency curve of induction propulsion motors and propellers.

The torque of one of the propellers ($T_p$) generates a total load on EPS and requires appropriate power from EPS, which simultaneously meets the needs of consumers. The load is connected to the switchboards of own needs and consumes the corresponding current within 20 % of the total current ($I$). The GA rotation frequency is represented in rad/sec and corresponds to the predefined speed equal to the rated power. The voltage at the DC link and the associated control input indicate the stability of the voltage when the load changes.
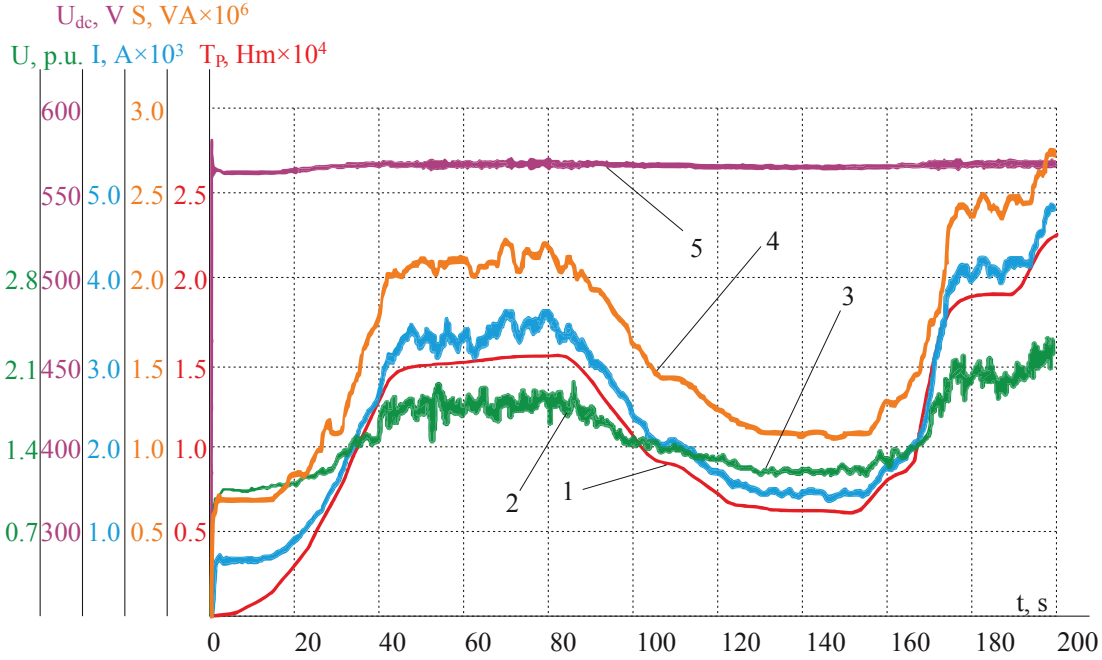
Fig. 2. EPS characteristics in different regions during the movement of a vessel: 1 — the torque on the shaft of the propulsion electric motor, $Nm \times 10^4$; 2 — GA excitation voltage, a.u.; 3 — total load current, $A \times 10^3$; 4 — total generated capacity, taking into consideration the work of EPS on CPH, $VA \times 10^6$; 5 — voltage at the *DC-Link*, V

**5. 2. Evaluation of variances in the deviation of parameters of the electric power system and control signals if a situational error occurs**

Similarly to (2), expressions for determining the variance of EPS power and the GA excitation voltage when adjusting the magnetic flux of GA in the function of the power of EPS on CPH take the form:

$$D_{S(p)} = \int_0^\infty \left| \frac{U + j\omega_{dg}}{Z(j\omega_{dg})} \right|^2 S_\mu(\omega_{dg}) d\omega, \qquad (20)$$

$$D_{U(p)} =$$
$$= \int_0^\infty \left| \frac{G(j\omega_{dg})(U + j\omega_{dg})}{Z(j\omega_{dg})N(j\omega_{dg})} - \frac{R(j\omega_{dg})}{N(j\omega_{dg})} \right|^2 S_\mu(\omega_{dg}) d\omega. \qquad (21)$$

Expressions for EPS with a DC link in a general form differ from expressions (2), (20), (21) only by the marks used.

The numerical values of polynomial coefficients included in expressions (8) to (10) and variances (2), (20), (21) are determined by intermediate values of the power value according to the available discrete set of CPH tasks. The conversion of the coordinates of the propulsion motor occurs at known time constants and transfer coefficients $k_{11}$, $k_{12}$, $k_{21}$, and $k_{22}$. The power limit is determined by the constraint on the control system, and the coefficient of decline and resonant frequency in expression (7) vary depending on the operating mode within the characteristic limits. Therefore, to assess the effectiveness of optimal control and determine the settings for optimal EPS controllers, it is necessary to obtain a series of dependences:

$$D_u = f\left(D_{ui}, \mu, \omega_{dg}, \delta_{dg}\right), \quad D_i = f\left(D_{U_p}, \mu, \omega_{dg}, \delta_{dg}\right),$$

$$D_\upsilon = f\left(\mu, \omega_{dg}, \delta_{dg}\right).$$

To determine the characteristics for the control signals of the optimal controller of the frequency of rotation and excitation voltage of EPS GA, it is necessary to calculate two laws: one to regulate the speed, and the second for the current excitation current. Obviously, moving thru iterative approximations, after sampling the coefficients of the GA speed control regulator, the following task for the excitation voltage controller is defined:

$$S_1^j\left(\dot{\zeta}_1^1\right): \min_{\upsilon_1^j}\left(U_N\left(\dot{\zeta}_1^1, \upsilon_1^j\right)\right) =$$
$$= \sum_{i=k}^{k+N-1} S\left(\dot{\zeta}_1^1(i), \omega_{ref}^j(i), \upsilon_1^j(i)\right) + S_f\left(\dot{\zeta}_1^1(k+N)\right).$$

Taking into consideration (11) for the steady regime of EPS GA and taking into consideration the following boundary conditions:

$$\dot{\zeta}_{1\min}^1 \le \dot{\zeta}_1^1\left(k_i+1\right) \le \dot{\zeta}_{1\min}^1;$$

$$\upsilon_{1\min}^1\left(k_i+i-1\right) \le \upsilon_1^j\left(k_i+i-1\right) \le \upsilon_{1\max}^1\left(k_i+i-1\right);$$

$$\forall i \in \left(0, N\right), \qquad (22)$$

where $U_N$ is a characteristic function of the projected EPS model; $N$ is the "horizon" of forecasting, $k$ is a discrete time step of modeling the system with the sample time $T \le$ time constant $T_{dg}$.

Fig. 3 shows the experimental characteristics of GA operation under the conditions of changing the load on EPS that works on CPH. The process of unsuccessful synchronization is registered using the standard EPS control algorithm implemented in DEIF PPM-3 controllers. Fig. 3 demonstrates that immediately after the GA is included in parallel operation, the system becomes unstable: there are fluctuations in the full (yellow plot) and active (green plot) loads; and, after a short period, the control system disconnects GA No. 1 from the buses of the main switchboard (MSB).

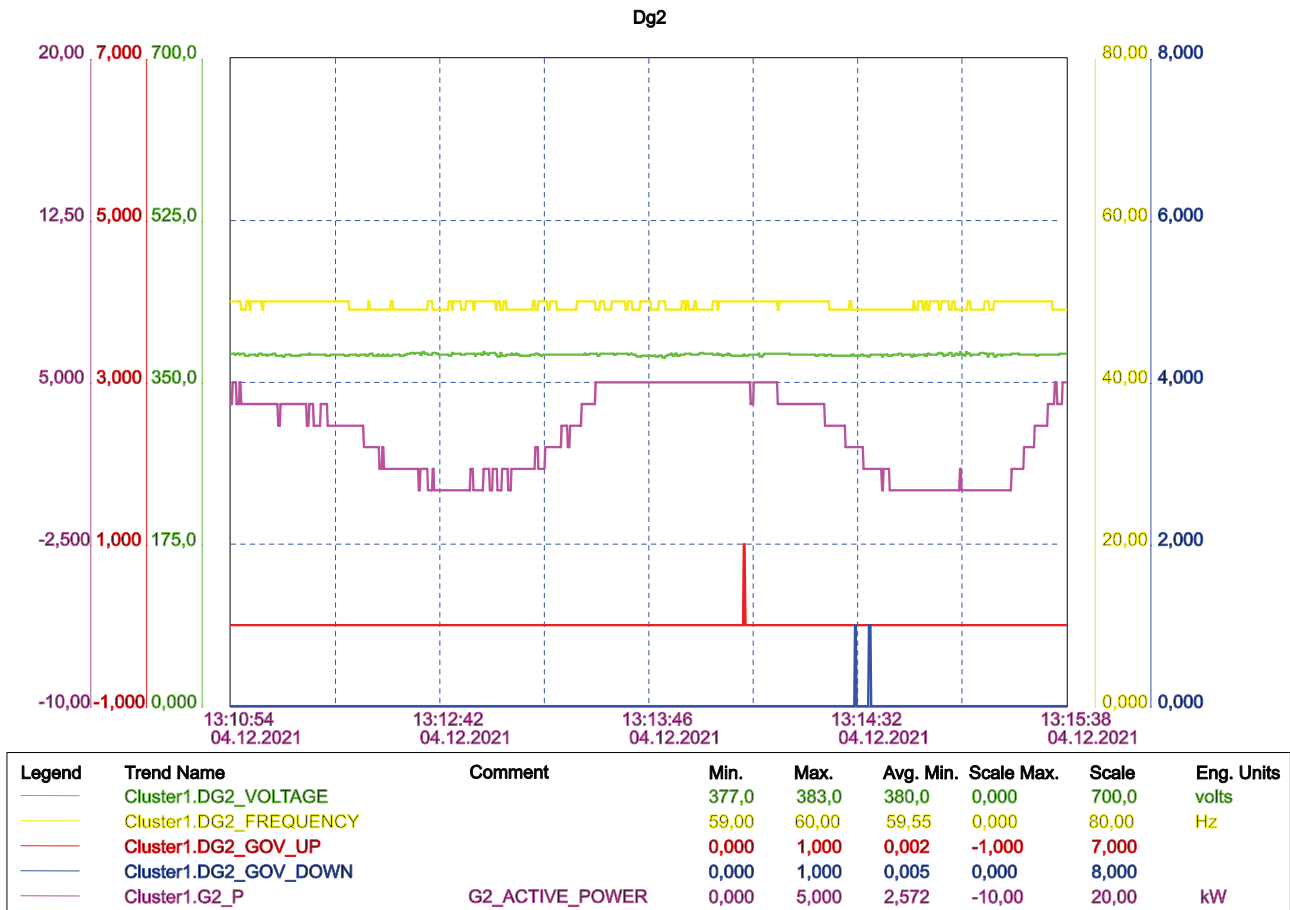| Legend | Trend Name | Comment | Min. | Max. | Avg. Min. | Scale Max. | Scale | Eng. Units |
|---|---|---|---|---|---|---|---|---|
| | Cluster1.DG2_VOLTAGE | | 377,0 | 383,0 | 380,0 | 0,000 | 700,0 | volts |
| | Cluster1.DG2_FREQUENCY | | 59,00 | 60,00 | 59,55 | 0,000 | 80,00 | Hz |
| | Cluster1.DG2_GOV_UP | | 0,000 | 1,000 | 0,002 | -1,000 | 7,000 | |
| | Cluster1.DG2_GOV_DOWN | | 0,000 | 1,000 | 0,005 | 0,000 | 8,000 | |
| | Cluster1.G2_P | G2_ACTIVE_POWER | 0,000 | 5,000 | 2,572 | -10,00 | 20,00 | kW |

Fig. 3. Experimental characteristics of generator assemblies under the conditions of changing the load on the electric power system

In a given case, there was an observation on similar samples, as, in relation to each other, two data flows change – the characteristics of EPS (Fig. 2) and the experimental characteristics of GA operation (Fig. 3). It was found that, at moments when the values in the flow of characteristics of EPS (Fig. 2) increase, the values for the GA entering the sub-synchronous rotation frequency in the stream of the experimental characteristics of GA operation (Fig. 3) (with a forward shift of 1 second) tend to decrease.

## 6. Discussion of the study into the optimization of the control system in an electric power system operating on a constant-power hyperbola

In comparison with the traditional methods to control EPS GA operating on CPH, the built algorithms are based on the correlation of the dynamics of the values of time constant of EPS links with the coefficients corresponding to control parameters (12). In some cases, when the exact parameters of the models are not available or their measurement is not possible, the data were filtered by the criterion of significance to a certain operational situation in terms of avoiding situational errors. Therefore, unlike known solutions [16–18], for such cases, the integral component (17) was taken into consideration in the control system. The result was achieved since the significance coefficients were calculated taking into consideration the integral condition for controlling voltage and rotation frequency.

Table 1 helps determine the values for control tasks $\mu(t)$ depending on the type of GA and an excitation system, as

well as possible reconstruction aspects. It should also be noted that for brushless turbocharged GAs, there are some restrictions on the excitation current due to a reduced air gap.

Our optimization of the system of EPS dynamics equations in accordance with the structure and settings of the optimal controller has proven the reliability of the probability of determining the occurrence of a situational error using correlation analysis. However, when analyzing Fig. 2, it should be noted that a situational error may occur due to inconsistencies in the subsystems of the general control system, in particular during the synchronization of EPS GA (Fig. 3). This disadvantage is a consequence of the fact that not all excitation systems make it possible to take into consideration the parameterization procedures for a certain operating mode.

The next stage of research is the algorithmization of EPS functioning in each isolated case. For formalization, it is necessary to use automatic languages – graphic, logical, matrix schemes of algorithms (GSA, LSA, ISA) or network graphs, which provide for a compact notation while maintaining full informativeness. In general, the functioning of EPS could be represented in the form of resulting functions followed by subsequent correlation analyses of the occurrence of a situational error in accordance with a certain operational regime.

The analysis of variance's methodology was implemented by acquiring data based on two streams: the characteristics of EPS (Fig. 2) and the experimental characteristics of GA operation (Fig. 3). In total, the data from 10 experiments in connecting GA to parallel work were analyzed, in particular, in the period of 344 seconds from 13.10.54 to 13.15.38 (04.12.2021) (Fig. 3). After filtering the data, the

sample was 200 seconds in accordance with Fig. 2, which is enough to identify a statistically significant correlation.

To identify the correlation between the characteristics of EPS (Fig. 2) and the experimental characteristics of GA operation, the value of the Spearman coefficient was calculated. It was 0.4263, at P-value – 0.0299. The method of linear regression was used to calculate the impact coefficient, which is –3.1204. The confidence interval at the level of significance of 0.05 is (–6.6207, 0.3798). This study's result established a negative correlation between variables over the specified period. In comparison with known approaches [40], the Shidak-Holm method was applied to introduce a correction to multiple hypothesis testing, and the P-value was less than the limit of 0.05. This makes it possible to avoid a certain number of iterative calculations, which, in turn, if one interprets these calculations as a mathematical component of the control system, hypothetically improves its performance. Therefore, the correlation between the characteristics of EPS and the values for GA entering the sub-synchronous rotation frequency in the stream of the experimental characteristics of GA (with a forward shift of 1 second) was recognized as statistically significant. The correlation is considered valid if Spearman's coefficient≥0.4.

The limitation of this study relates to that the homoscedasticity of the data was assessed as the absence of heteroscedasticity based on the analysis of the dependent characteristics of EPS and independent variables (the power for own needs).

Further studies should involve comparing experimental data with empirical decomposition of modeling results in the time space of the occurrence of situational errors. This could reduce variational components as undetected in non-recursive algorithms with feedback failure for a certain parameter. The task to preliminary determine the number of levels in the decomposition of a control signal in terms of significance could be solved by determining the dominant real signal with an improvement in the signal/error ratio.

## 7. Conclusions

1. The occurrence of a situational error during the synchronization of EPS GA was compensated by optimizing the system of EPS dynamics equations in accordance with the structure and settings of the optimal controller. The EPS power controller was tested under the mode of changing the load of own needs with the power levels of EPS on CPH in the range of 50–100 % of the rated one. When the EPS power controller was turned on during the synchronization of GA,

there was a significant decrease in the fluctuations in current consumption and load. When turning on the EPS rotation frequency controller, the stable operation of GA, close to the mode of operation on CPH, was ensured. In comparison with the traditional methods to control EPS GA on CPH, the built algorithms are based on the correlation of the dynamics of the values of time constants of EPS links with coefficients corresponding to control parameters. The result was achieved due to the calculation of significance coefficients, taking into consideration the integral condition for controlling the voltage and rotation frequency with the corresponding correlation to the integral component in the control system. The optimization of the system of EPS dynamics equations in accordance with the structure and settings of the optimal controller has proven the reliability of the probability of determining the occurrence of a situational error using correlation analysis. Situational errors due to inconsistencies in the subsystems of the general control system during the synchronization of EPS GA remain a consequence of the impossibility of taking into consideration the procedures for parameterizing excitation systems under a certain operational mode.

2. Variances in the deviation of parameters of the electric power system and control signals, subject to the appearance of a situational error, were determined during physical modeling:
– of the long-term EPS operation for different levels of power for own needs;
– of the slow increase and decrease in the torque on the shaft of the propulsion engine in the range from idle to rated;
– of the sudden torque surge on the propulsion motor according to different values of the average period of oscillations in the propeller torque.

With slow transitions of EPS from one mode of operation to another by changing the torque of the propeller, the task signal forming device provides automatic reconfiguration of the feedback coefficients $k_{11}$, $k_{12}$, $k_{21,}$ and $k_{22}$ to a new mode. Moreover, the speed of reconfiguration should not exceed the time constants of voltage controllers and GA rotation frequency, depending on the mode of operation of EPS and the level of power for own needs. In the case of sudden surges in the torque, the excitation voltage controller provides forcing of the magnetic flux of GA, and the power controller provides stabilization of EPS power. The range of deviations of the current consumed at the enabled GA rotation controller was 10 % of the average value. The range of power deviations of EPS with the power controller turned on was 5 %. Integration of the proposed control law with active filter control systems to compensate for higher voltage harmonics and current of electrical networks could improve the quality of electricity of autonomous EPSs in the combined propulsion complexes.

References

1. Haseltalab, A., Wani, F., Negenborn, R. R. (2022). Multi-level model predictive control for all-electric ships with hybrid power generation. International Journal of Electrical Power & Energy Systems, 135, 107484. doi: https://doi.org/10.1016/j.ijepes.2021.107484

2. Boričić, A., Torres, J. L. R., Popov, M. (2021). Fundamental study on the influence of dynamic load and distributed energy resources on power system short-term voltage stability. International Journal of Electrical Power & Energy Systems, 131, 107141. doi: https://doi.org/10.1016/j.ijepes.2021.107141

3. Ortega, Á., Milano, F. (2019). Voltage Stability of Converter-Interfaced Energy Storage Systems. IFAC-PapersOnLine, 52 (4), 222–227. doi: https://doi.org/10.1016/j.ifacol.2019.08.187

4. Soomro, A. H., Larik, A. S., Mahar, M. A., Sahito, A. A., Soomro, A. M., Kaloi, G. S. (2021). Dynamic Voltage Restorer – A comprehensive review. Energy Reports, 7, 6786–6805. doi: https://doi.org/10.1016/j.egyr.2021.09.004

5. Chen, Y., Huang, Z. (2014). A High Performance Computing Platform for Performing High-Volume Studies with Windows-based Power Grid Tools. IFAC Proceedings Volumes, 47 (3), 10772–10777. doi: https://doi.org/10.3182/20140824-6-za-1003.00839

6. Neuman, P. (2009). Models of synchronous generator and transformers for Dispatch Training Simulators and Real Time Digital Simulators. IFAC Proceedings Volumes, 42 (9), 398–403. doi: https://doi.org/10.3182/20090705-4-sf-2005.00070

7. The RTDS Simulator is the world's benchmark for real-time power system simulation. Available at: https://www.rtds.com/

8. Budashko, V., Shevchenko, V. (2021). The synthesis of control system to synchronize ship generator assemblies. Eastern-European Journal of Enterprise Technologies, 1 (2 (109)), 45–63. doi: https://doi.org/10.15587/1729-4061.2021.225517

9. Nivelo, J. J. O., Coello, J. A. C., Pereira, G. G. C., Passos, F. O., Filho, J. M. C., Guerrero, C. A. V. et. al. (2021). Evaluating voltage drop snapshot and time motor starting study methodologies – An offshore platform case study. Electric Power Systems Research, 196, 107187. doi: https://doi.org/10.1016/j.epsr.2021.107187

10. Hvozdeva, I., Myrhorod, V., Budashko, V., Shevchenko, V. (2020). Problems of Improving the Diagnostic Systems of Marine Diesel Generator Sets. 2020 IEEE 15th International Conference on Advanced Trends in Radioelectronics, Telecommunications and Computer Engineering (TCSET). doi: https://doi.org/10.1109/tcset49122.2020.235453

11. Vitalii, B., Vitalii, N., Mark, N., Sergii, K. (2018). Parametrization and identification of energy flows in the ship propulsion complex. 2018 14th International Conference on Advanced Trends in Radioelecrtronics, Telecommunications and Computer Engineering (TCSET). doi: https://doi.org/10.1109/tcset.2018.8336205

12. Myrhorod, V., Hvozdeva, I., Budashko, V. (2020). Multi-parameter Diagnostic Model of the Technical Conditions Changes of Ship Diesel Generator Sets. 2020 IEEE Problems of Automated Electrodrive. Theory and Practice (PAEP). doi: https://doi.org/10.1109/paep49887.2020.9240905

13. Budashko, V., Shevchenko, V. (2021). Solving a task of coordinated control over a ship automated electric power system under a changing load. Eastern-European Journal of Enterprise Technologies, 2 (2 (110)), 54–70. doi: https://doi.org/10.15587/1729-4061.2021.229033

14. Van den Broeck, G., Stuyts, J., Driesen, J. (2018). A critical review of power quality standards and definitions applied to DC microgrids. Applied Energy, 229, 281–288. doi: https://doi.org/10.1016/j.apenergy.2018.07.058

15. Budashko, V. V. (2017). Design of the three-level multicriterial strategy of hybrid marine power plant control for a combined propulsion complex. Electrical Engineering & Electromechanics, 2, 62–72. doi: https://doi.org/10.20998/2074-272x.2017.2.10

16. Balog, R. S., Weaver, W. W., Krein, P. T. (2012). The Load as an Energy Asset in a Distributed DC SmartGrid Architecture. IEEE Transactions on Smart Grid, 3 (1), 253–260. doi: https://doi.org/10.1109/tsg.2011.2167722

17. Lu, X., Sun, K., Guerrero, J. M., Vasquez, J. C., Huang, L., Wang, J. (2015). Stability Enhancement Based on Virtual Impedance for DC Microgrids With Constant Power Loads. IEEE Transactions on Smart Grid, 6 (6), 2770–2783. doi: https://doi.org/10.1109/tsg.2015.2455017

18. Kwasinski, A., Onwuchekwa, C. N. (2011). Dynamic Behavior and Stabilization of DC Microgrids With Instantaneous Constant-Power Loads. IEEE Transactions on Power Electronics, 26 (3), 822–834. doi: https://doi.org/10.1109/tpel.2010.2091285

19. Feng, X., Ye, Z., Xing, K., Lee, F. C., Borojevic, D. (1999). Impedance specification and impedance improvement for DC distributed power system. 30th Annual IEEE Power Electronics Specialists Conference. Record. (Cat. No.99CH36321). doi: https://doi.org/10.1109/pesc.1999.785616

20. Beires, P., Vasconcelos, M. H., Moreira, C. L., Peças Lopes, J. A. (2018). Stability of autonomous power systems with reversible hydro power plants. Electric Power Systems Research, 158, 1–14. doi: https://doi.org/10.1016/j.epsr.2017.12.028

21. Xie, P., Tan, S., Guerrero, J. M., Vasquez, J. C. (2021). MPC-informed ECMS based real-time power management strategy for hybrid electric ship. Energy Reports, 7, 126–133. doi: https://doi.org/10.1016/j.egyr.2021.02.013

22. Gaber, M., El-Banna, S. H., El-Dabah, M., Hamad, M. S. (2021). Intelligent Energy Management System for an all-electric ship based on adaptive neuro-fuzzy inference system. Energy Reports, 7, 7989–7998. doi: https://doi.org/10.1016/j.egyr.2021.06.054

23. Kemmetmüller, W., Eberharter, S., Kugi, A. (2014). Quasi optimal feedforward control of a very low frequency high-voltage test system. IFAC Proceedings Volumes, 47 (3), 11623–11628. doi: https://doi.org/10.3182/20140824-6-za-1003.00356

24. Watari, D., Taniguchi, I., Goverde, H., Manganiello, P., Shirazi, E., Catthoor, F., Onoye, T. (2021). Multi-time scale energy management framework for smart PV systems mixing fast and slow dynamics. Applied Energy, 289, 116671. doi: https://doi.org/10.1016/j.apenergy.2021.116671

25. Payvand, B., Hosseini, S. M. H. (2019). A new method for mitigating frequency fluctuations in ships with electrical propulsion. ISA Transactions. doi: https://doi.org/10.1016/j.isatra.2019.02.013

26. Chaal, M., Valdez Banda, O. A., Glomsrud, J. A., Basnet, S., Hirdaris, S., Kujala, P. (2020). A framework to model the STPA hierarchical control structure of an autonomous ship. Safety Science, 132, 104939. doi: https://doi.org/10.1016/j.ssci.2020.104939

27. Geertsma, R. D., Negenborn, R. R., Visser, K., Hopman, J. J. (2017). Design and control of hybrid power and propulsion systems for smart ships: A review of developments. Applied Energy, 194, 30–54. doi: https://doi.org/10.1016/j.apenergy.2017.02.060

28. Azizi, A., Peyghami, S., Mokhtari, H., Blaabjerg, F. (2019). Autonomous and decentralized load sharing and energy management approach for DC microgrids. Electric Power Systems Research, 177, 106009. doi: https://doi.org/10.1016/j.epsr.2019.106009

29. Yuan, Y., Wang, J., Yan, X., Shen, B., Long, T. (2020). A review of multi-energy hybrid power system for ships. Renewable and Sustainable Energy Reviews, 132, 110081. doi: https://doi.org/10.1016/j.rser.2020.110081

30. Adamson, G., Holm, M., Moore, P., Wang, L. (2016). A Cloud Service Control Approach for Distributed and Adaptive Equipment Control in Cloud Environments. Procedia CIRP, 41, 644–649. doi: https://doi.org/10.1016/j.procir.2015.12.020

31. Naik, K. R., Rajpathak, B., Mitra, A., Kolhe, M. L. (2021). Adaptive energy management strategy for sustainable voltage control of PV-hydro-battery integrated DC microgrid. Journal of Cleaner Production, 315, 128102. doi: https://doi.org/10.1016/j.jclepro.2021.128102

32. Marqusee, J., Becker, W., Ericson, S. (2021). Resilience and economics of microgrids with PV, battery storage, and networked diesel generators. Advances in Applied Energy, 3, 100049. doi: https://doi.org/10.1016/j.adapen.2021.100049

33. Kusakaka, K., Phiri, S. F., Numbi, B. P. (2021). Optimal energy management of a hybrid diesel generator and battery supplying a RTG crane with energy recovery capability. Energy Reports, 7, 4769–4778. doi: https://doi.org/10.1016/j.egyr.2021.07.074

34. Zhang, C., Jia, B. (2019). Research on Energy Efficiency Optimization Strategy of Electric Propulsion Ships with Energy Storage Devices. 2019 Chinese Automation Congress (CAC). doi: https://doi.org/10.1109/cac48633.2019.8997039

35. Longva, T., Eide, M. S., Skjong, R. (2010). Determining a required energy efficiency design index level for new ships based on a cost-effectiveness criterion. Maritime Policy & Management, 37 (2), 129–143. doi: https://doi.org/10.1080/03088830903533759

36. Glavatskhih, V., Lapkin, A., Dmitrieva, L., Khodikova, I., Golovin, A. (2021). Ships' energy efficiency management: organizational and economic aspect. MATEC Web of Conferences, 339, 01020. doi: https://doi.org/10.1051/matecconf/202133901020

37. Budashko, V., Shevchenko, V. (2018). Synthesis of the Management Strategy of the Ship Power Plant for the Combined Propulsion Complex. 2018 IEEE 5th International Conference on Methods and Systems of Navigation and Motion Control (MSNMC). doi: https://doi.org/10.1109/msnmc.2018.8576266

38. Budashko, V., Golikov, V. (2017). Theoretical-applied aspects of the composition of regression models for combined propulsion complexes based on data of experimental research. Eastern-European Journal of Enterprise Technologies, 4 (3 (88)), 11–20. doi: https://doi.org/10.15587/1729-4061.2017.107244

39. Budashko, V. V. (2017). Pidvyshchennia efektyvnosti funktsionuvannia sudnovykh enerhetychnykh ustanovok kombinovanykh propulsyvnykh kompleksiv. Odessa. Available at: http://www.onma.edu.ua/wp-content/uploads/2016/09/Thesis_Budashko_END-1.pdf

40. Yang, H., Cheng, Y., Li, G. (2021). A denoising method for ship radiated noise based on Spearman variational mode decomposition, spatial-dependence recurrence sample entropy, improved wavelet threshold denoising, and Savitzky-Golay filter. Alexandria Engineering Journal, 60 (3), 3379–3400. doi: https://doi.org/10.1016/j.aej.2021.01.055